应用超常介质设计柱形隐形容器*

马越界[1],黄建平[2],孙文波[3,4],刘德全[5]

(1 鄂尔多斯气象局,鄂尔多斯 017000;2 兰州大学大气科学学院,兰州 730000;3 汉普顿大学大气科学中心,弗吉尼亚 23668;4 美国国家航空航天局朗利研究中心,弗吉尼亚 23681-2199;5 兰州大学物理学院,兰州 730000)

摘要　超常介质是一种纳米尺度的人工复合材料,可以同时设定材料的介电常数和磁导率。利用超常介质的这一特性,能够自由地调整光的传播路径。在此基础上,应用坐标转换的方法,计算出圆柱形和椭圆柱形的介电常数和磁导率分布,让光在介质内沿着特定的轨迹传播,绕过包围的空腔,沿入射的方向出射,从而实现圆柱和椭圆柱形状的隐形。

关键词　超常介质　坐标转换　柱形隐形容器

中图分类号:O439　　文献标识码:A

Design Column Cloak Using Metamaterial

MA Yuejie[1], HUANG Jianping[2], SUN Wenbo[3,4], LIU Dequan[5]

(1 Erdos City Bureau of Meteorology, Erdos 017000;2 College of Atmosphere Sciences, Lanzhou University, Lanzhou 730000; 3 The National Center for Atmospheric Research, Hampton University, VA 23668;4 Langley Research Center, National Aeronautics and Space Administration, VA 23681-2199;5 College of Physics, Lanzhou University, Lanzhou 730000)

Abstract　Metamaterial, a kind of artificial material composed by nanometer units, can be controlled permittivity and permeability at the same time, Taking advantage of this finding, we can adjust the transmission of light. We used the approach of transformation optics and calculated out the permittivity and permeability of Metamaterial cloak in the condition of cylindrical and elliptical cylinder, to make sure the light along the specific trajectory and spread around the cloak, then outgoing along the direction of the incident radiation. In this way, the information inside the cloak can not be divulged.

Key words　metamaterial, transformation optics, column type cloak

超常介质是一种纳米尺度的人工复合材料,通常由纳米微杆、金属小环等构成其结构单元,这些纳米小部件在材料中扮演着人造原子的角色。最常见的结构单元是裂环金属共振器结构[1,2]:由一个有缝隙的传导金属环组成,缝隙的目的是提供电容。这些机构单元的尺度要小于目的波长,因而会产生一些奇特的电磁性质。由于纳米工艺技术的进步,可以把这些纳米结构单元做得很小,从而在微观尺度上实现自然存在的介质所没有的性质,如实现负折射率[3-6]、使材料的磁导率不为 1[5]等。由于超常介质在国防、科研等方面的应用,引起国内外研究者的广泛关注,但以往的研究主要以球形为主[7,8],限制了其应用。本研究利用坐标转换的方法,计算出圆柱形和椭圆柱形的介电常数和磁导率分布,让光在介质内沿着特定的轨迹传播,绕过包围的空腔,沿入射的方向出射,从而实现圆柱和椭圆柱形状的隐形。

1　光线垂直圆柱体入射

运用超常介质可以自由地设定介电常数和磁导率[5]的特性,可以控制光的传播速度和传播方向,以实现隐形:控制光经过隐形容器介质层,绕过空腔,出射时光的传播方向、相位和入射光相同。这样容器所盛物体的信息不会通过光传播出去。图 1 为光束垂直入射圆柱形隐形容器的坐标变换示意图。

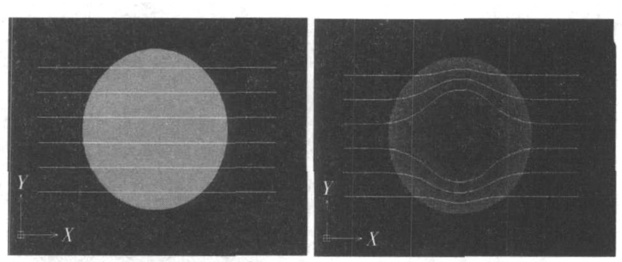

(a)未经‘拉伸’时光束通过均匀介质轨迹图　　(b)‘拉伸’后的光束垂直入射圆柱形隐形容器轨迹图

图 1　光束垂直入射圆柱形隐形容器的坐标变换示意图

Fig. 1　The diagram about coordinate transformation of light normally incident beaming cylindrical

为了将这一过程形象化,假设系统处在一个可以随意拉伸的介质内如图 1(a)所示。记录下笛卡尔网格中的初始

*国家杰出青年科学基金(40725015)

马越界:男,1985 年生,硕士研究生,主要从事星载云雷达的资料分析研究　E-mail:Mayuan456123@163.com

场[3]，设线元为 x、y、z。然后，将柱体进行拉伸，变为如图1(b)所示的形状，设此时的坐标系的线元为 q_1、q_2、q_3，则弧元的关系为[1]：

$$ds^2 = dx^2 + dy^2 + dz^2 = Q_{11}dq_1^2 + Q_{22}dq_2^2 + Q_{33}dq_3^2 + 2Q_{12}dq_1dq_2 + 2Q_{13}dq_1dq_3 + 2Q_{23}dq_2dq_3 \quad (1)$$

$$Q_{ij} = \frac{\partial x}{\partial q_i}\frac{\partial x}{\partial q_j} + \frac{\partial y}{\partial q_i}\frac{\partial y}{\partial q_j} + \frac{\partial z}{\partial q_i}\frac{\partial z}{\partial q_j} \quad (2)$$

简写 $Q_i^2 = Q_{ii}$。在新坐标系中，麦克斯韦方程组可写为：

$$(\nabla_q \times \hat{E})^i = -\mu_0 \sum_{j=1}^{3} \hat{\mu}^{ij} \frac{\partial \hat{H}_j}{\partial t}$$
$$(\nabla_q \times \hat{H})^i = +\varepsilon_0 \sum_{j=1}^{3} \hat{\mu}^{ij} \frac{\partial \hat{H}_j}{\partial t} \quad (3)$$

$$\hat{\mu}^{ij} = \mu\delta^{ij} Q_1Q_2Q_3(Q_iQ_j)^{-1}$$
$$\hat{\varepsilon}^{ij} = \varepsilon\delta^{ij} Q_1Q_2Q_3(Q_iQ_j)^{-1} \quad (4)$$

这样在新的坐标系下，介电常数和磁导率变为[1]：

$$\begin{cases} \varepsilon_{q_n}{}' = \varepsilon_{q_n} \dfrac{Q_{q_1}Q_{q_2}Q_{q_3}}{Q_{q_n}^2} \\ \mu_{q_n}{}' = \mu_{q_n} \dfrac{Q_{q_1}Q_{q_2}Q_{q_3}}{Q_{q_n}^2} \qquad n = 1,2,3 \\ E_{q_n}{}' = Q_{q_n}E_{q_n}, H_{q_n}{}' = Q_{q_n}H_{q_n} \end{cases} \quad (5)$$

如图2(a)所示，在柱坐标系下：

$$x = r\cos\theta$$
$$y = r\sin\theta \quad (6)$$
$$z = z$$

设经过拉伸后柱形介质的横截面内径为 R_1，外径为 R_2，如图2(b)所示。经过拉伸，介质的横截面径长由 r 变为 r'，其中 $r=0$ 拉伸到 $r'=R_1$，$r=R_2$ 拉伸到 $r'=R_2$。

假设 r 和 r' 之间的关系是线性的，从而新坐标为：

$$r' = R_1 + \frac{r(R_2 - R_1)}{R_2}$$
$$\theta' = \theta, z' = z \quad (7)$$

代入式(2)得：

$$Q_{r'}{}^2 = \left(\frac{\partial x}{\partial r}\frac{\partial r}{\partial r'}\right)^2 + \left(\frac{\partial y}{\partial r}\frac{\partial r}{\partial r'}\right)^2 + \left(\frac{\partial z}{\partial r}\frac{\partial r}{\partial r'}\right)^2 = \left(\cos\theta\frac{R_2}{R_2 - R_1}\right)^2 + \left(\sin\theta\frac{R_2}{R_2 - R_1}\right)^2 + 0 = \left(\frac{R_2}{R_2 - R_1}\right)^2 \quad (8)$$

$$Q_{\theta'}{}^2 = \left(\frac{\partial x}{r'\partial\theta'}\right)^2 + \left(\frac{\partial y}{r'\partial\theta'}\right)^2 + \left(\frac{\partial z}{r'\partial\theta'}\right)^2 = \left(-\frac{r^2}{r'^2}\sin\theta\right)^2 + \left(\frac{r^2}{r'^2}\cos\theta\right)^2 + 0 = \frac{r^2}{r'^2} \quad (9)$$

$$Q_{z'}{}^2 = \left(\frac{\partial x}{\partial z'}\right)^2 + \left(\frac{\partial y}{\partial z'}\right)^2 + \left(\frac{\partial z}{\partial z'}\right)^2 = 0^2 + 0^2 + 1 = 1 \quad (10)$$

代入式(5)可得光垂直入射时圆柱形隐形容器的介电常数和磁导率的分布为：

$$\varepsilon_{r'} = \mu_{r'} = \frac{R_2 - R_1}{R_2}\frac{r}{r'}$$
$$\varepsilon_{\theta'} = \mu_{\theta'} = \frac{R_2}{R_2 - R_1}\frac{r'}{r}$$
$$\varepsilon_{z'} = \mu_{z'} = \frac{R_2}{R_2 - R_1}\frac{r}{r'}$$

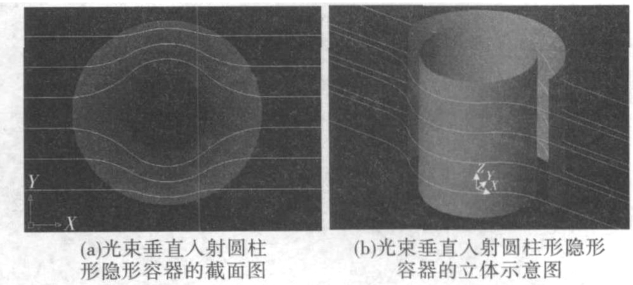

图2 圆柱体下光垂直柱轴入射的轨迹示意图

Fig. 2 The diagram about light normally incident beaming the cylinder

2 光线斜入射圆柱形隐形容器

光线斜入射圆柱形隐形容器时，可以看作是垂直入射等偏心率的椭圆柱，如图3所示。

设光线入射面于水平面的夹角为 α，椭圆的长轴方向为 x 方向，在柱坐标系下，线元 x、y、z 分别为：

$$x = \frac{r\cos\theta}{\cos\alpha}$$
$$y = r\sin\theta \quad (11)$$
$$z = z$$

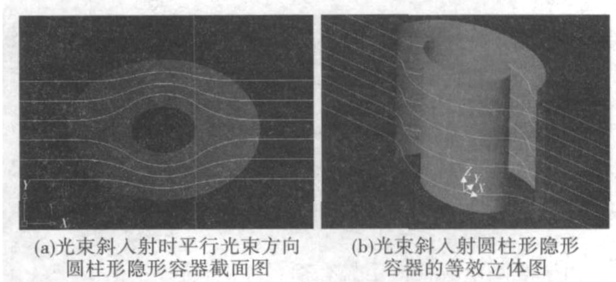

图3 光束斜入射圆柱形隐形容器的等效轨迹示意图

Fig. 3 The diagram about light oblique incident beaming the cylinder

利用以上的变化方法，经过拉伸后：

$$r' = R_1 + \frac{r(R_2 - R_1)}{R_2}$$
$$\theta' = \theta, z' = z \quad (12)$$

于是得出在光线斜入射圆柱形隐形容器的介电常数和磁导率分布：

$$\varepsilon_{r'} = \mu_{r'} = \frac{\sqrt{\left(\dfrac{R_2}{R_2 - R_1}\right)^2\dfrac{\cos^2\theta}{\cos^2\alpha} + \left(\dfrac{R_2}{R_2 - R_1}\right)^2\sin^2\theta} \cdot \sqrt{\dfrac{r^2}{r'^2\cos^2\alpha}\sin^2\theta + \dfrac{r^2}{r'^2}\cos^2\theta}}{\left(\dfrac{R_2}{R_2 - R_1}\right)^2\dfrac{\cos^2\theta}{\cos^2\alpha} + \left(\dfrac{R_2}{R_2 - R_1}\right)^2\sin^2\theta}$$

$$\varepsilon_{\theta'}=\mu_{\theta'}=\frac{\sqrt{(\frac{R_2}{R_2-R_1})^2\frac{\cos^2\theta}{\cos^2\alpha}+(\frac{R_2}{R_2-R_1})^2\sin^2\theta}\cdot\sqrt{\frac{r^2}{r'^2\cos^2\alpha}\sin^2\theta+\frac{r^2}{r'^2}\cos^2\theta}}{\frac{r^2}{r'^2\cos^2\alpha}\sin^2\theta+\frac{r^2}{r'^2}\cos^2\theta}$$

$$\varepsilon_{z'}=\mu_{z'}=\sqrt{(\frac{R_2}{R_2-R_1})^2\frac{\cos^2\theta}{\cos^2\alpha}+(\frac{R_2}{R_2-R_1})^2\sin^2\theta}\cdot\sqrt{\frac{r^2}{r'^2\cos^2\alpha}\sin^2\theta+\frac{r^2}{r'^2}\cos^2\theta}$$

3　光沿椭圆长轴方向垂直入射椭圆柱形隐形容器(内层为圆柱形)

光线沿椭圆长轴方向垂直入射椭圆柱形隐形容器(内层为圆柱形)时如图 4 所示。

在柱坐标系下:

$$x=\alpha r\cos\theta$$
$$y=r\sin\theta \qquad (13)$$
$$z=z$$

设外层椭圆横截面的长短周分别为 a 和 b,沿着椭圆柱形的长轴方向,在椭圆柱形截面的内边界 $r'=R$,在截面的外边界 $r'=a$,从而可以得到权重系数 $\alpha=b/a$。

经变换为:

$$\begin{cases}x=(1+\frac{\frac{b}{a}-1}{a}r)r\cos\theta\\ y=r\sin\theta\\ z=z\end{cases}\qquad(14)$$

$$r'=R+\frac{r(a-R)}{R},\theta'=\theta,z'=z\qquad(15)$$

$$Q_{r'}=\sqrt{(\frac{a}{a-R})^2+(2\frac{(b-a)r}{a(a-R)}\cos\theta)^2}$$

$$Q_{\theta'}=\sqrt{(\frac{r}{r'})^2+(\frac{b-a}{a^2}\frac{r^2}{r'}\sin\theta)^2}$$

$$Q_{z'}=1$$

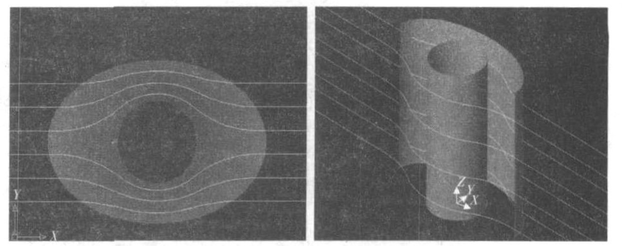

(a)平行光束方向椭圆柱形隐形容器截面示意图　　(b)椭圆柱形隐形容器立体示意图

图 4　光线沿椭圆长轴方向垂直入射椭圆柱轨迹示意图(内层为圆柱)

Fig. 4　The diagram about light normally incident beaming the elliptical cylinder

代入式(5)得:

$$\varepsilon_{r'}=\mu_{r'}=\frac{\sqrt{(\frac{a}{a-R})^2+(2\frac{(b-a)(r'-R)}{(a-R)^2}\cos\theta)^2}\cdot\sqrt{(\frac{(r'-R)a}{r'(a-R)})^2+(\frac{(b-a)(r'-R)^2}{r'(a-R)^2}\sin\theta)^2}}{(\frac{a}{a-R})^2+(2\frac{(b-a)(r'-R)}{(a-R)^2}\cos\theta)^2}$$

$$\varepsilon_{\theta'}=\mu_{\theta'}=\frac{\sqrt{(\frac{a}{a-R})^2+(2\frac{(b-a)(r'-R)}{(a-R)^2}\cos\theta)^2}\cdot\sqrt{(\frac{(r'-R)a}{r'(a-R)})^2+(\frac{(b-a)(r'-R)^2}{r'(a-R)^2}\sin\theta)^2}}{(\frac{(r'-R)a}{r'(a-R)})^2+(\frac{(b-a)(r'-R)^2}{r'(a-R)^2}\sin\theta)^2}$$

$$\varepsilon_{z'}=\mu_{z'}=\sqrt{(\frac{a}{a-R})^2+(2\frac{(b-a)(r'-R)}{(a-R)^2}\cos\theta)^2}\cdot\sqrt{(\frac{(r'-R)a}{r'(a-R)})^2+(\frac{(b-a)(r'-R)^2}{r'(a-R)^2}\sin\theta)^2}$$

由于椭圆空心柱体不具有轴对称性,所以它的式子变得如此复杂。实际制作中,可以在小范围内取近似值,而不是让它们的值非常精确地按连续函数变化。每一束进入柱体的光线都沿着一条相对应的曲线绕过空腔,相比未对空腔区域拉伸前,光程变长了。为了隐藏空腔内的信息,在光程变长的同时,光从介质内出射时的相速要与入射时相同。这就意味着相速大于光在真空中的传播速度。而如果同时要求光束没有色散,这样群速和相速相等,且群速不得能超过光速。因此在这种方法中,必须要求材料对频率产生色散,而这样最终符合条件的只是特定的光的频率[9-11]。

4　结论

超常介质可以在很小范围内任意调节介电常数和磁导率,因此可以自由地设计材料的介电常数和磁导率,应用坐标转换的方法,计算出圆柱形和椭圆柱形隐形容器的介电常数和磁导率分布,实现了从圆形到柱形隐形容器的突破。实际制作中,可以在小范围内近似地取 $\varepsilon_{r'}$、$\varepsilon_{\theta'}$、$\varepsilon_{z'}$、$\mu_{r'}$、$\mu_{\theta'}$、$\mu_{z'}$ 的值,而不是让它们值非常精确地按连续函数变化。从以上的计算可以看出,运用坐标转换的方法,设计的容器尺寸没有严格的限定,对于所要隐藏的物体也没有要求,因为它的应用十分广泛,如设计隐形衣、保护光敏材料等。运用该方法,还可以对其它具有超对称结构的形状进行类似的形状衍生,构建更复杂形状的隐形容器,从而使隐形容器的应用从单一的球形向多种形状拓展,为隐形容器的广泛应用提供参考。

参考文献

1　Schurig D, Mock J J, Justice B J, et al. Electromagnetic cloak at microwave frequencies[J]. Science, 2006, 314(5801):977

(下转第 79 页)

参考文献

1 Gray J E, Luan B. Protective coatings on magnesium and its alloys-A critical reviews[J]. J Alloy Compd, 2002, 336(1-2):88

2 Fukuda H, Matsumoto Y. Effects of Na_2SiO_3 on anodization of Mg-Al-Zn alloy in 3 M KOH solution[J]. Corros Sci, 2004, 46(9):2135

3 Barnes T A, Pashby I R. Joining techniques for aluminium space frames used in automobiles. Part Ⅱ. Adhesive bonding and mechanical fasteners[J]. J Mater Process Techn, 2000, 99(1-3):72

4 Critchlow G W, Yendall K A, Bahrani D, et al. Strategies for the replacement of chromic acid anodising for the structural bonding of aluminium alloys[J]. Int J Adhes Adhes, 2006, 26(6):419

5 Cai Q Z, Wang L S, Wei B K, et al. Electrochemical performance of microarc oxidation films formed on AZ91D magnesium alloy in silicate and phosphate electrolytes[J]. Surf Coat Techn, 2006, 200(12-13):3727

6 Bala Srinivasan P, Blawert C, Dietzel W. Effect of plasma electrolytic oxidation treatment on the corrosion and stress corrosion cracking behaviour of AM50 magnesium alloy[J]. Mater Sci Eng A, 2008, 494(1-2):401

7 Chang L M. Growth regularity of ceramic coating on magnesium alloy by plasma electrolytic oxidation[J]. J Alloy Compd, 2009, 468(1-2):462

8 Jin F, Chu P K, Xu G D. Structure and mechanical properties of magnesium alloy treated by micro-arc discharge oxidation using direct current and high-frequency bipolar pulsing modes[J]. Mater Sci Eng A, 2006, 435-436:123

9 Zhang R F, Shan D Y, Chen R S, et al. Effects of electric parameters on properties of anodic coatings formed on magnesium alloys[J]. Mater Chem Phys, 2008, 107(2-3):356

10 Lv G H, Chen H, Gu W C, et al. Effects of current frequency on the structural characteristics and corrosion property of ceramic coatings formed on magnesium alloy by PEO technology[J]. J Mater Process Techn, 2008, 208(1-3):9

11 Packham D E. Surface energy, surface topography and adhesion[J]. Int J Adhes Adhes, 2003, 23(6):437

12 Jiang Z X, Huang Y D, Liu L, et al. Effects of roughness on interfacial performances of silica glass and non-polar polyarylacetylene resin composites[J]. Appl Surf Sci, 2007, 253(24):9357

13 Critchlow G W, Brewis D M. Review of surface pretreatments for aluminium alloys[J]. Int J Adhes Adhes, 1996, 16(4):255

14 Jiang Bailing(蒋百灵), Wu Guojian(吴国建), Zhang Shufen(张淑芬), et al. Research on micromechanism and growth procedure of ceramic coating formed by micro-arc oxidation on magnesium alloys(镁合金微弧氧化陶瓷层生长过程及微观结构的研究)[J]. Trans Metal Heat Treatment(金属热处理学报), 2002, 23(1):5

15 Chen Xianming(陈显明), Luo Chengping(罗承萍), Liu Jiangwen(刘江文), et al. Structure of ceramic coating produced by micro-arc oxidation on Mg alloy(镁合金微弧氧化膜层结构)[J]. J Central South University: Sci Techn(中南大学学报:自然科学版), 2006, 37(6):1065

16 Chen Dongchu(陈东初), Li Wenfang(李文芳), Jie Jun(揭军), et al. Micro-structure and composition of ceramic coating on AZ91D magnesium alloy prepared by micro-arc oxidation(AZ91D 镁合金表面微弧氧化陶瓷膜微观结构与组成的研究)[J]. Rare Metal Mater Eng(稀有金属材料与工程), 2009, 38(S2):731

(责任编辑 赵海艳)

(上接第 62 页)

2 Gabielli L H, Jaime Cardenas, Carl B Poitras, et al. Silicon nanostructure cloak operating at optical frequencies[J]. Nature Photonics, 2009, 3(8):461

3 Shalaev V M. Optical negative-index metamaterials[J]. Nature Photonics, 2007, 1(1):41

4 Plum E, Zhou J, Dong J, et al. Metamaterial with negative index due to chiarlity[J]. Phys Rev B, 2009, 79(3):035407

5 Padilla W J, Taylor A J, Highstrete C, et al. Dynamical electric and magnetic metamaterial response at terahertz frequencies[J]. Phys Rev Lett, 2006, 96(10):107401

6 Yen T J, Padilla W J, Fang N, et al. Terahertz magnetic response from artificial materials[J]. Science, 2004, 303(5663):1494

7 Pendry J B, Schurig D, Smith D R. Controlling electromagnetic fields[J]. Science, 2006, 312(5781):1780

8 Hu T, Landy N I, Fan K, et al. Flexible terahertz metamaterials: Towards a terahertz metamaterial invisible cloak[C]. Technical Digest-Internationa Electron Devices Meeting, 2008

9 Wood B, Pendry J B. Metamaterials at zero frequency[J]. J Phys: Condensed Matter, 2007, 19(7):076208

10 Dolling G, Wegener M, Soukoulis C M, et al. Negativeindex metamaterial at 780nm wavelength[J]. Opt Lett, 2007, 32(1):53

11 Stefan Linden L, Christian E, Martin W, et al. Magnetic response of metamaterialst 100 terahertz[J]. Science, 2004, 306(5700):1351

(责任编辑 云 哲)